Geofísica Internacional
ISSN: 0016-7169
silvia@geofisica.unam.mx
Universidad Nacional Autónoma de México
México

Imhof, Armando Luis; Santamarina, Juan Carlos

Seismic parameter evaluation of gravel and sand samples subjected to stress using general purpose piezocrystals

Geofísica Internacional, vol. 51, núm. 2, abril-junio, 2012, pp. 109-119
Universidad Nacional Autónoma de México
Distrito Federal, México

Geofísica Internacional (2012) 51-2: 109-119

Original paper

Seismic parameter evaluation of gravel and sand samples subjected to stress using general purpose piezocrystals

Armando Luis Imhof* and Juan Carlos Santamarina

Received: April 25, 2008; accepted: January 6, 2011; published on line: March 30, 2012

Resumen

Se presenta el desarrollo e implementación de técnicas geofísicas altamente resolutivas basadas en la transmisión de ondas elásticas en gravas y arenas secas mediante el empleo de instrumental de bajo costo desarrollado para este estudio. Las técnicas fueron aplicadas en muestras de arenas y gravas a escala de laboratorio con diferentes grados de compactación. La adquisición de datos se efectuó utilizando piezocristales de muy bajo costo como emisores y receptores de señales, y otros dispositivos sencillos tales como microprocesadores TL084 como amplificadores analógicos. Como sismógrafo y convertidor A-D de las señales se empleó un osciloscopio Tektronix TDS 210 con capacidad de almacenamiento de datos en PC. Las muestras fueron sometidas a varios estados de esfuerzo con el propósito de simular profundidades crecientes. Se observó una correlación marcada entre las velocidades de propagación V_P y los espectros de frecuencia con los esfuerzos efectivos aplicados que reflejaron el carácter inherentemente no-lineal de los contactos entre partículas, tal como lo describe el modelo hertziano. Durante el ciclo de descarga, los valores de V_P fueron mayores que los correspondientes al ciclo inicial de carga, debido a la reubicación (y compactación) de los granos durante el mismo. Por consiguiente es posible conocer el estado de compactación de las partículas en una muestra dada estudiando las propagación de ondas sísmicas, las cuales se calculan *antes* y *después* de la carga.

Palabras clave: piezocristales, esfuerzos efectivos, ondas sísmicas, palanca, pulser, osciloscopio.

Abstract

High resolution geophysical techniques based on the transmission of elastic waves in dry samples of gravels and sands were developed and implemented. Laboratory specimens of alluvial sand and gravel were prepared at different compaction levels. Low cost piezocrystals transducers were used as sources and receivers; and TL084 microprocessors as analog amplifiers. A TDS 210 Tektronix digital oscilloscope was used for A-D conversion. The specimens were subjected to stress simulating sediments at different subsurface depths. Propagation velocity, V_P and frequency spectra were found to correlate with the applied effective stress and reflected non-linear inter-particle contact response. During the discharge cycle, V_P values exceeded those of the initial load cycle, as grains were relocated and compacted in the loading process. Thus, compaction in a given sample may be obtained from seismic waves propagation, *before* and *after* loading.

Key words: piezocrystals, effective stress, seismic waves, crowbar press, pulser, oscilloscope.

A. L. Imhof
Instituto Geofísico Sismológico Volponi
Facultad de Ciencias Exactas Físicas y Naturales
Universidad de San Juan
San Juan, Argentina
*Corresponding author: aimhof@unsj.edu.ar

J. C. Santamarina
Center for Applied Geomaterials Research
Georgia Institute of Technology
Atlanta, Georgia, USA

Introduction

Geophysical techniques based on the transmission of elastic waves may be developed using a low-cost device. The techniques were applied to sand and gravel samples prepared in the laboratory.

Frequency behaviour and velocity-stress relationship in stressed soils led to the following empirical expressions (Roesler, 1990; Yu and Richart, 1984; Santamarina and Potts, 1994):

$$V_P^x = \alpha \left(\frac{\sigma'_x}{1atm} \right)^{\beta} \qquad \alpha, \beta \ constants \tag{1}$$

$$V_S^{x,y} = \eta \left(\frac{\sigma'_x}{1atm} \right)^{\delta} \cdot \left(\frac{\sigma'_y}{1atm} \right)^{\theta}$$

$$\eta, \delta, \theta \ constants \tag{2}$$

where *P* and *S* waves propagate along the *x* direction, *S* is *y* polarized, and σ'_x and σ'_y are the effective stresses in *x* and *y*.

Geophysical tests of granular media in the laboratory scale faces challenges such as transducer-medium coupling, difficulties in source design, selection of receiving transducers, inherent dispersion, and selective attenuation of frequencies as a function of wavelength λ and particle size. Seismic wave propagation in granular materials at low strains allows for non-destructive, *in situ* characterization of alluvial gravel and sand deposits.

Instrumentation

General purpose piezocrystals of disk cell type (APCI, 2000) measuring 20 mm in diameter were used as sources and receivers (Figure 1-a). The crystal vibrates at resonant frequency under an electric impulse (Wells, 1977). Resonant frequency is inversely proportional to thickness of the piezoelectric material (approximately λ/2). The bandwidth is also inversely related to duration of excitation (Lee, 2003).

The electrical pulse differs from the mechanical true signal emitted by the transducer. Therefore, the output needs to be monitored. This is done by joining two crystals; one that transforms electric signal into mechanical, and the other that converts mechanical form into electrical one and transmits it to the DSO. Figure 1-b shows the connection scheme and Figure 2 depicts the actual form of the output pulse and its frequency content.

System Assembly: Cell and System Connection

Figure 3 shows the cylindrical steel cell (V_{steel}=6,000m/s; Santamarina *et al.*, 2001), containing the samples and the outline of the system.

A "pulser" was built as signal generator to trigger impulses of short duration (10μs) in periodic form, every 10 ms at high amplitudes (40 to 400 V).

An operational amplifier FET TL084 of up to 80 dB gain was connected to the PZT receiver and fed at 12 VCC, through a 100 Hz high-pass

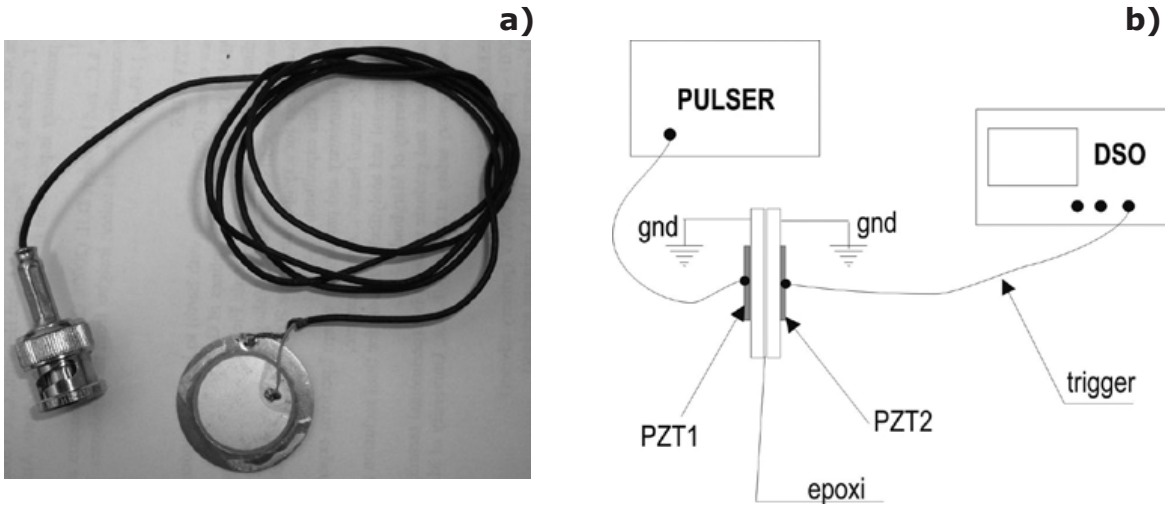

Figure 1. (a) Disk Cells. (b) Connection of transducers to Pulser and DSO for real transmitted wave monitoring.

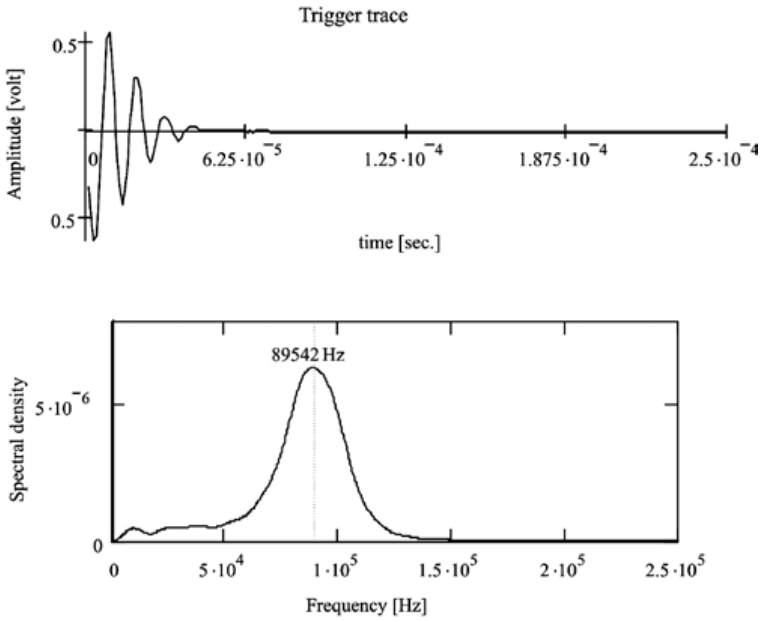

Figure 2. Output Signal from pulser. (a) Real output wave. (b) Power density of it.

filter. A two channel 60 MHz real-time digital oscilloscope TEKTRONIX TDS 210 (DSO) with external trigger was used as a seismograph, with a sampling rate of up to 1 G samples.

The DSO has an RS232 interface. A BASIC algorithm was designed and implemented for transferring data to the PC for signal processing.

General purpose piezoelectric ceramics of 4.1 kHz of resonance frequency transducers were employed as wave source *E* and receiver *R*.

Direct Arrivals

To calculate the transmission velocities, it is necessary to accurately determine the first arrivals (direct waves). Therefore, it is essential to know the types of possible arrivals in the confined media in order to eliminate the non-direct waves.

Imhof (2007) studied wave propagation inside cylindrical test steel probes. Direct, refracted and transmitted waves propagate through the cell walls. It was observed that (a) waves transmitted by the walls arrive much faster than the others due to the high propagation velocity. The base and the cover were isolated with rubber O-rings to decouple the waves; (b) for distances H>0.13 m and diameter ϕ = 0.125 m, the refracted waves will reach *R* earlier. To avoid this, the E-R distance for the tests was selected at H = 0.1m.

System Assembly: Crowbar Press

A lever structure was designed and constructed in order to apply weights in increments, thus multiplying the force *Ft* up to about 50 times. Figure 4 shows the crowbar press structure. *F1* represents the incrementing weights at the end of the crowbar. The relationship between *Ft* and *F1* can be expressed as:

$$Ft \cdot a = F1 \cdot L\,(a) = F1 \cdot 48.4\,a \qquad (3)$$

The cell containing the sample covered with a cap was placed below the point of *Ft* application, enabling high stress application.

Table 1. Volumetric Form and Shallow Texture of Soil Samples Used. (Courtesy: Instituto de Materiales y Suelos, FI-UNSJ).

SIZE	PARTICLE DIAMETER	ESFERICITY	TEXTURE
#20 - #50	0.841 mm - 0.297 mm	0.8	subrounded
#8 - #20	2.38 mm - 0.841 mm	0.7	subangled to subrounded

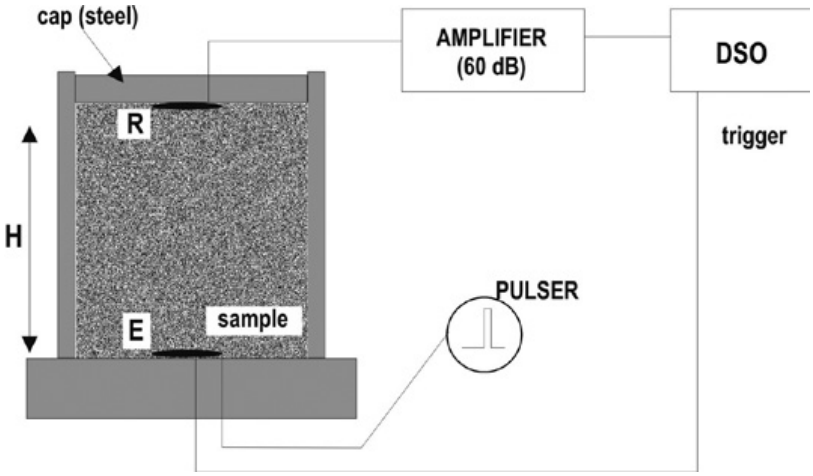

Figure 3. Cilindric cell for tests and connection scheme.

Methodology

Tests were carried out on two dry samples of sand and gravel (SP and GP; USCS-ASTM) of different grain sizes (#20 - #50 and #8 - #20, ASTM). Table 1 summarizes the sample characteristics. Tests for sand samples (SP) of grain size about 0.297 mm (#50) and 0.841 mm (#20) were performed. The same procedure was repeated for the second set of samples.

Two packing forms were considered: Loose *A*, poured using a tablespoon, ensuring greatest volume of holes among the grains, maximizing the pore space; and Compact *C,* compressing it mechanically in order to minimize the pore space without breaking the grains.

The sample was placed inside the test cell (Figure 3) at a distance H=0.1m. The coupled PZT (source *E* and trigger) was mounted on the base, and the material was covered with a steel cap. The core of the receiving PZT was fixed with epoxy elastic mastic and connected to the DSO through the amplification system. Force was applied through *Ft* (Figure 4). Once the first measurement was obtained and recorded, *Ft* was successively incremented by *F1* up to the maximum load possible; followed by gradual unloading.

All measurements were transmitted to a PC through the RS232 interface. The signal to noise relationship was improved using 128 stacks in order to randomly cancel or minimize the noise, thereby enhancing the incoming signal.

The confined effective stress σ' was incremented using the values presented in Table 2 by adding successive weights through F1. This

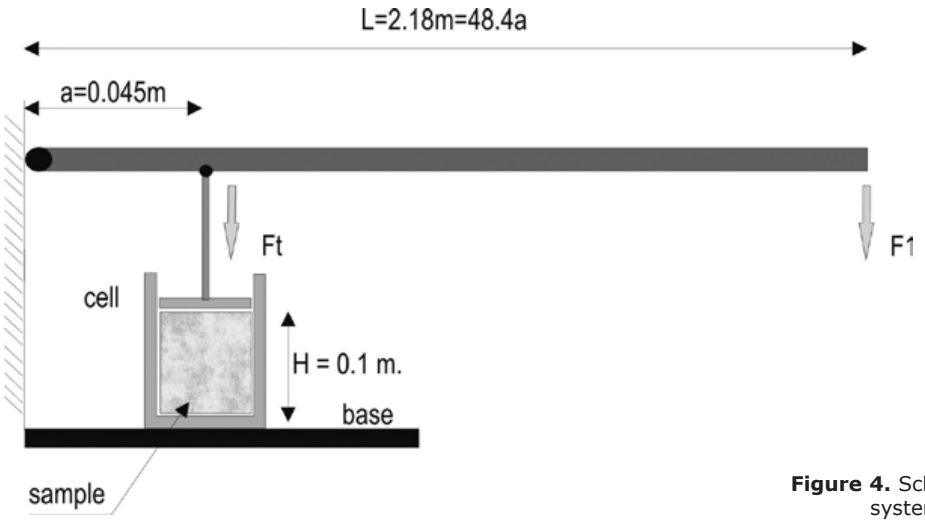

Figure 4. Schematic of crowbar press system and probe cell.

Table 2. Load regime in cell probe and equivalent calculated soil depths.

Cell Loads			
Cell Area (m^2)	*Ft* [*N*]*acum*	σ'[*kPa*]	*z equiv*[*m*]
0,0123	10	0,81	0,05
0,0123	30	2,44	0,14
0,0123	60	4,88	0,28
0,0123	100	8,13	0,46
0,0123	180	14,63	0,83
0,0123	405	32,93	1,87
0,0123	2940	239,02	13,54
0,0123	4634	376,75	21,34
0,0123	5844	475,12	26,92
0,0123	7780	632,52	35,83
0,0123	12620	1026,02	58,12
0,0123	17460	1419,51	80,41
0,0123	21816	1773,66	100,48

Table also shows the equivalent soil depths of the stress, with a normal density δ=1.8 kg/dm^3 (Hough, 1957; Sharma, 1997).

The above procedure was repeated for all samples and for all compaction types.

Results

Figures 5 (a) and 6 (a) show the arrival times of waves for samples #20-#50 (A) and #8-#20 (A) with cell loads. Arrival time decreases with increased loading which causes an increase in the velocity of propagation (V_P). In addition, arrival time during unloading is lower than during loading. This results in an increase in V_P at the end of the complete cycle (hysteresis). This phenomenon can also be observed in the compacted samples.

Figures 5 (b) and 6 (b) show the spectral densities of the two samples under different load states. The bandwidth increases with effective

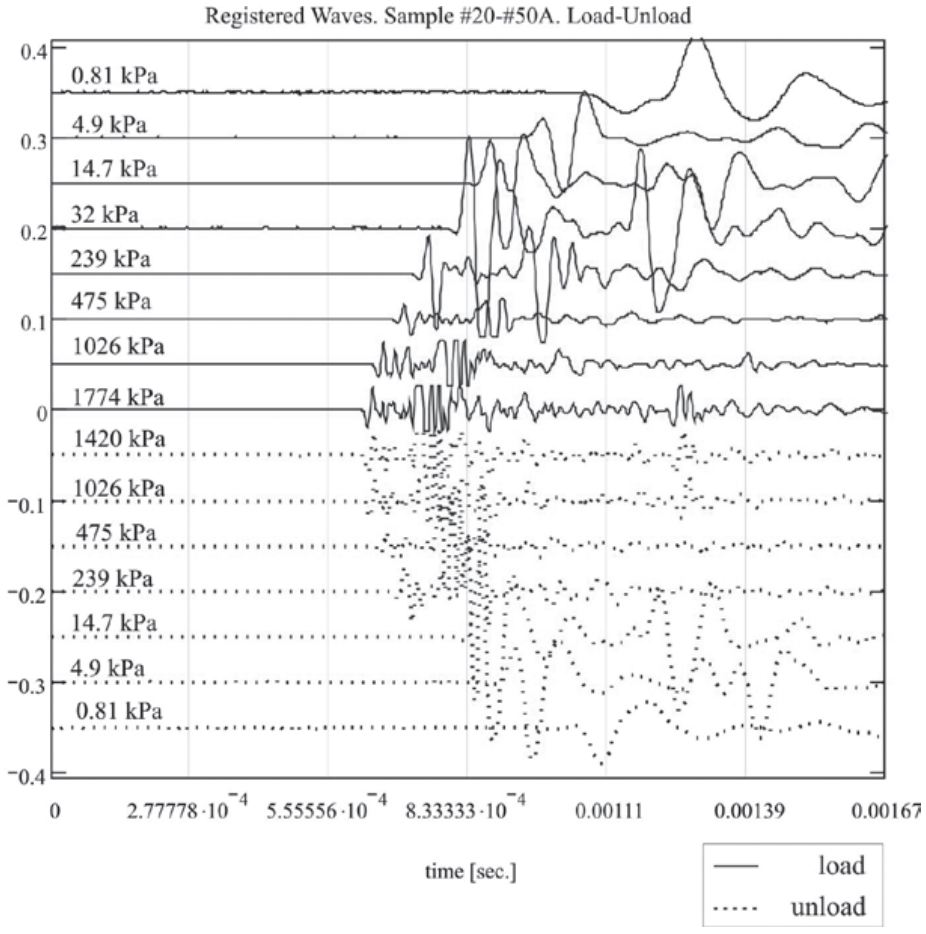

Figure 5a. Registered Waves (a) and Power Spectra (b). Sample #20 - #50 (A).

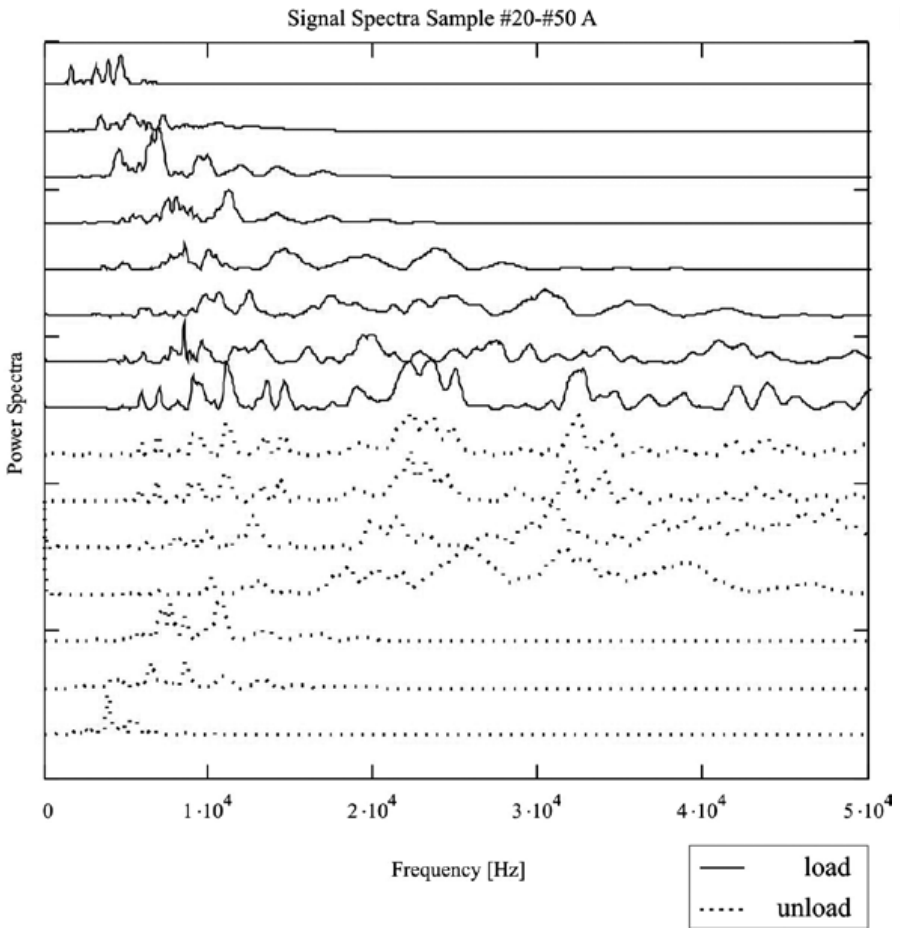

stress, most likely due to an increase in contact surface among particles (strain) which is produced by an increase in the confining pressure, and hence the granular rearrangement. The pore space diminishes, and the sample behaves more like a continuous one, decreasing the selective attenuation of frequencies.

After unloading, the bandwidth peaks of the two samples shift to the right (higher frequencies) due to the modified granular rearrangement (hysteresis).

Finally, the maximum amplitude peaks are greater after the loading cycle due to improvement in transducer coupling.

Figure 7 (a-b) shows the σ' - V_p diagram for samples #20-#50A and #8-#20A respectively for both the loading and unloading cycles. V_p varies in the interval 180-820 m/s (finer sample) and 196-920 m/s (coarser sample). All these show that velocities are greater at unloading; in case of the loose sample, a more drastic initial reduction occurs in pore space.

Both figures show a logarithmic behaviour, starting with abrupt increments of V_p for small σ', with initial propagation velocities of approximately 200 m/s. This could be attributed to significant grain rearrangement at the beginning of the load cycle. Hence, even under small loads, we can observe an abrupt decrease in pore space and an increment in the contact surface of the particles (large slope). This variation decreases afterwards; V_p tends to stabilize and approaches a constant value, even under notable increase in stress (low slope).

It is important to define the approximate point where the velocity changes abruptly. From this point on, the stress dependent heterogeneity tends to be constant (and hence V_p). Thus we may apply ray theory from inversion problems (*e.g.* tomography). Figure 8 (a-b) shows the previous graph in a semi-log scale (corresponding to loading cycle only). In order to predict V_p for other depths (within the interval considered), fitting curves were calculated for both cases.

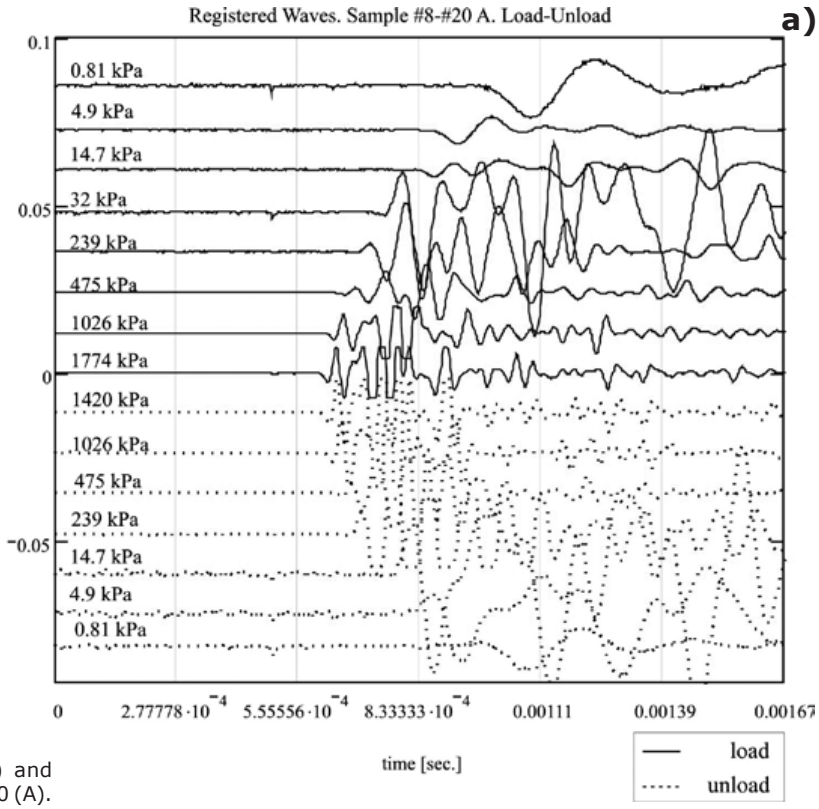

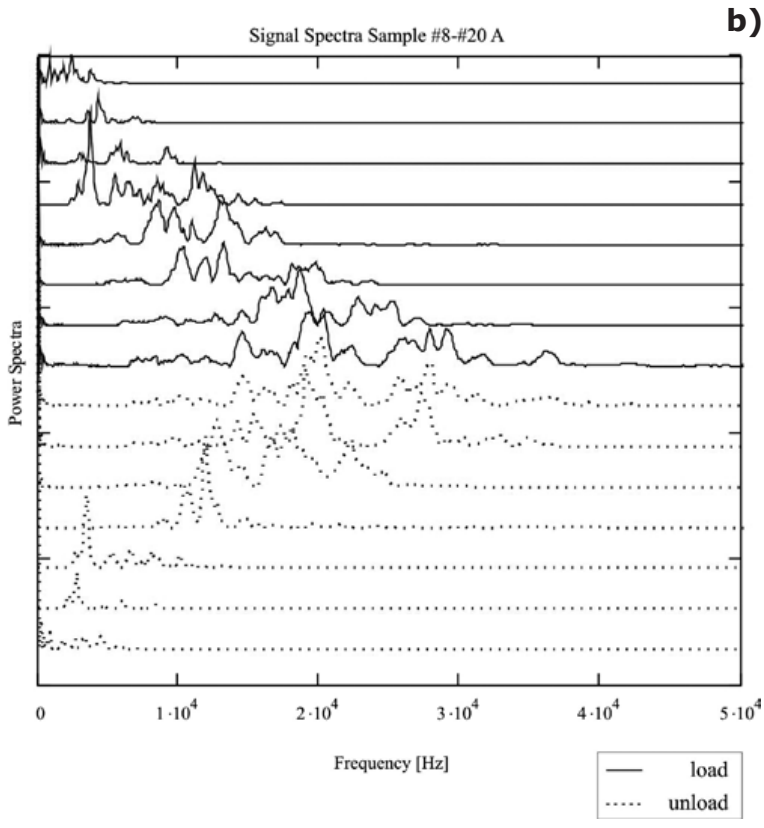

Figure 6. Registered Waves (a) and Power Spectra (b). Sample #8 - #20 (A).

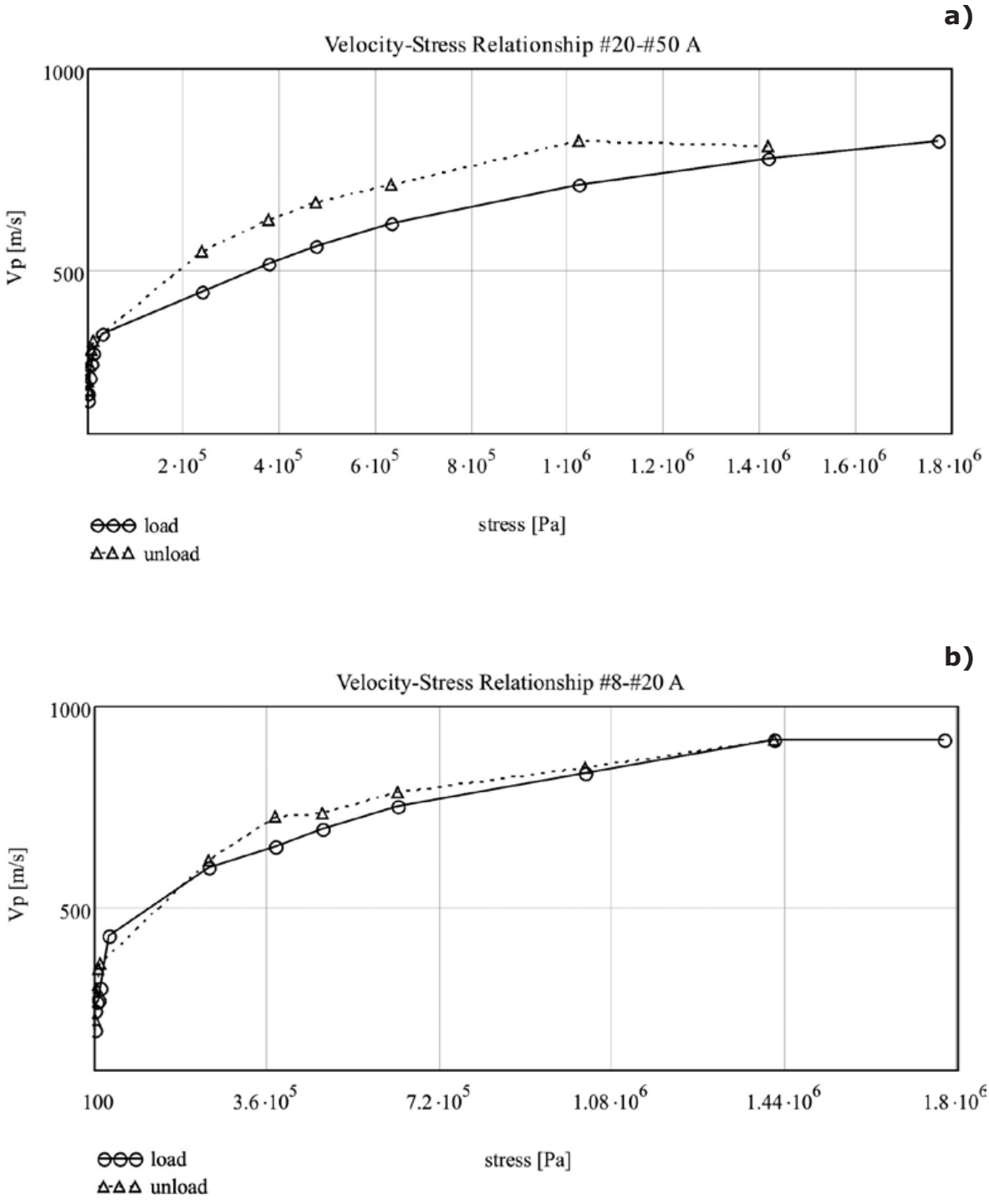

Figure 7. V_p - σ′ relationship. Load and Unload. (a) #20-#50 A sample; (b) #8-#20 A sample.

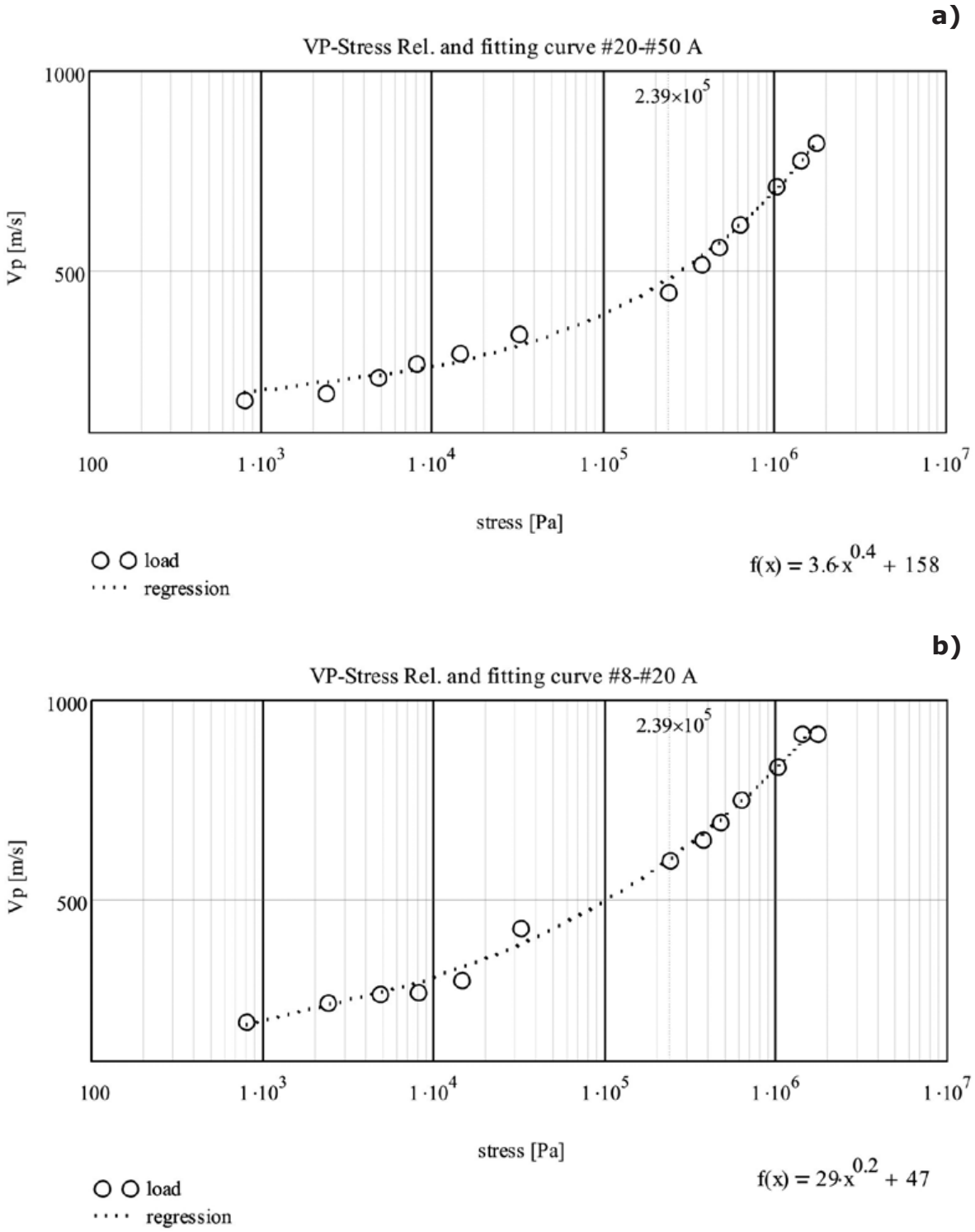

Figure 8. V_p -σ' relationship. Fitting functions. (a) #20-#50 A sample; (b) #8-#20 A sample.

The inflection point where V_p changes abruptly is about 239 kPa corresponding to a depth of 13 m. This value is significant because tomographic inversion schemes using straight rays can be used *beyond* this depth. For shallower depths, ray bending (curved ray-theory) must be used. This increases the level of complexity because of the introduction of non-linearity.

Also, the granular rearrangement stops near the inflection point (not considering crushing). Beyond this point the velocity increases in smaller degree despite the large increments in pressure, up to approximately 900 m/s for both samples. This will remain almost constant until the crushing threshold produced by stress is reached.

Conclusions

Novel characterization methods may be useful in geotechnics. The methodology presented in this paper uses general purpose electronic devices for data acquisition, storage and processing. Piezocrystals, digitizers and computers facilitated the development of advanced sensing technology for engineering applications at low cost.

1. V_p increases abruptly for the initial load states because of grain rearrangement and increase in contact surface between particles. Further, the velocity gradient decays and reaches an approximate constant value.

2. During unloading, V_p is higher than during the initial loading cycle, because sample grains were rearranged. Therefore, it is possible to observe the compaction of particles in a given sample by studying the propagation of seismic waves *before* and *after* loading.

3. For depths of up to 100 m V_p increases with depth in coarse granular soils as a power of stress. The frequency spectrum moves toward high frequencies and the spectral density increases.

4. Significant non-linearity of V_p at shallow depths is observed. Therefore, the acoustic impedance also varies and produces heterogeneity and stress dependent anisotropy, which causes ray bending.

5. Propagation velocity changes with depth thus showing that the underground is not homogeneous. Therefore, the propagation of waves is neither spherical nor plane.

6. The resulting ray bending requires special consideration when studying shallow-depth tomographic inversions. The straight-ray theory should not be used.

7. The V_p's of the materials and their frequency spectra are correlated with the effective stresses. This is a direct consequence of the non-linear effect of the inter-particle contact (Hertzian contact).

8. The piezoelectric transducers can be subjected to high loads without depolarization or mechanical fracture. They support tensions of up to 400 V without breaking if the excitation is of short duration (e.g., 10 msec as verified, or less).

9. The increment of the confining pressure improves transducer-sample coupling.

Acknowledgements

This study was supported in part by the CICITCA project "Detección y Modelado de Inclusiones en Arena por Tomografía Sísmica en Cross Hole"; Universidad Nacional de San Juan (UNSJ), Argentina. Special thanks are due to Instituto de Materiales y Suelos, UNSJ for sample analysis.

Bibliography

American Piezo Com International, 2000, *Piezoelectric Ceramics: Principles and Applications.* APCI.

Hough B.K., 1957, Basic Soils Engineering. *The Ronald Press Co*. New York. 513 pág.

Imhof A.L., 2007, Caracterización de Arenas y Gravas con Ondas Elásticas por Tomografía Sísmica en Cross-Hole. *Ph.D. Thesis*. Universidad Nacional de Cuyo. Mendoza Argentina. International PHd Thesis Award, Fundación García Siñériz, XIV Convocatoria, Spain.

Lee J.S., 2003, High Resolution Geophysical Techniques For Small-Scale Soil Model Testing. *Ph.D. Thesis*. Georgia Institute of Technology. Atlanta. USA.

Roesler S.K., 1979, Anisotropic Shear Modulus Due to Stress Anisotropy. *ASCE. J. Geotechnical Engineering Division*. 105; 871-880.

Santamarina, J.C., Potts B., 1994, On the Imaging of Stress Changes in Particulate Media – An Experimental Study. *Canadian Geotechnical Journal*, vol. 31, n. 2, pp 215-222.

Santamarina J.C., Klein K.A., Fam M.A., 2001, Soils and Waves. *Wiley and Sons. Ltd. England*.

Sharma P.V., 1997, Environmental and Engineering Geophysics *1st Ed. Cambridge University Press*. Cambridge. 475 pág.

Wells P.N.T., 1977, Biomedical Ultrasonics. *Academic Press. New York*, 635 pp.

Yu P., Richart F.E., 1984, Stress Ratio Effects on Shear Modulus of Dry Sands. *ASCE. J. Geotechnical Engineering Division*. 110; 331-335.